NASA Technical Memorandum 86862

RF Sputtered Silicon and Hafnium Nitrides as Applied to 440C Steel

A. Grill
Ben Gurion University of the Negev
Beer Sheeva, Israel

and

P. R. Aron
Lewis Research Center
Cleveland, Ohio

March 1984

NASA

Completed 8/2/85

ERRATA

NASA Technical Memorandum 83592

RF SPUTTERED SILICON AND HAFNIUM NITRIDES AS APPLIED TO 440C STEEL

A. Grill and P. R. Aron
March 1984

Cover and report documentation page: The report number should be Technical Memorandum 86862.

RF SPUTTERED SILICON AND HAFNIUM NITRIDES AS APPLIED TO 440C STEEL

A. Grill
Ben Gurion University of the Negev
Beer Sheva, Israel

and

P. R. Aron
National Aeronautics and Space Administration
Lewis Research Center
Cleveland, Ohio

SUMMARY

Silicon nitride and hafnium nitride coatings were deposited by reactive rf sputtering on oxidized and unoxidized 440C stainless steel substrates. Sputtering was done in mixtures of argon and nitrogen gases from pressed powder silicon nitride and from hafnium metal targets. Depositions were at two background pressures, 8 and 20 mtorr, and at two different fractions (f) of nitrogen in argon, 0.25 and 0.60, for hafnium nitride and at f = 0.25 for silicon nitride. The coatings and the interface between the coating and substrate were investigated by X-ray diffractometry, scanning electron microscopy, energy dispersive X-ray analysis and Auger electron spectroscopy (AES). A Knoop microhardness of 1650±100 kg/mm^2 was measured for hafnium nitride and 3900±500 kg/mm^2 for silicon nitride. The friction coefficients between a 440C rider and the coatings were measured as lubricated with mineral oil and where found not to depend on the sputtering conditions. They varied between 0.33 and 0.56 for silicon nitride and between 0.42 and 0.73 for hafnium nitride. X-ray diffractometry revealed that the silicon nitride coatings were amorphous. The hafnium nitride coatings were composed of crystallites of mixed phases with a characteristic grain size of no less than 50 Å. The sample with f = 0.60 appeared to be predominately HfN while those with f = 0.25 appeared to be predominately Hf_4N_3. AES showed that the silicon nitride samples deposited at 20 mtorr contained significantly higher levels of oxygen and carbon than the 8 mtorr samples. Oxide was found at all interfaces with an interface width of at least 600 Å for the oxidized substrates and at least 300 Å for the unoxidized substrates. Scratch test results demonstrate that the adhesion of hafnium nitride to both oxidized and unoxidized 440C is superior to that of silicon nitride. Oxidized 440C is found to have increased adhesion, to both nitrides, over that of unoxidized 440C. Coatings of both nitrides deposited at 8 mtorr were found to have increased adhesion to both oxidized and unoxidized 440C over those deposited at 20 mtorr.

INTRODUCTION

The group IV nitrides are characterizied by chemical stability, good dielectric properties and high hardness, i.e., >2000 kg/mm (ref. 1). As a result, there has been a growing interest in the properties of and synthesis techniques for thin films of these materials. They are finding increasing application in the electronics industry (refs. 2 and 3), as decorative coatings (ref. 4), for solar cell applications (ref. 5) and as wear reducing coatings

for cutting tools (refs. 6 and 7). At this laboratory, in pursuit of the tribological properties of promising materials, a study of the characteristics of silicon and hafnium nitrides produced by reactive rf sputtering was begun. This technique offers the advantage of a relatively low substrate temperature. The dependence of the composition and rate of deposition on the concentration of nitrogen in the sputtering gas and on the sputtering pressure has been reported (refs. 8 and 9). It was found that the adherence of silicon nitride to 304 stainless steel improves with decreasing sputtering pressure. Since the adherence of the coatings is an important factor for practical applications, the study, focused on two materials, silicon nitride and hafnium nitride, is continued. Its goal is to gain a better understanding of the relationship between the deposition conditions, the structure and composition of the coatings and the interface, and their adherence to an important bearing material, hardened 440C stainless steel. It has been shown (ref. 10) that the adhesion of some hard coatings to this material is improved if the surface, of the substrate, is oxidized. Therefore, for the present study, both oxidized and unoxidized substrates are used.

EXPERIMENTAL CONDITIONS

The coatings were reactively deposited in a diode type rf sputtering system, shown schematically in figure 1. The system was operated, at 13.5 MHz, at an average power density of 2.7 watts/cm^2. The targets were 15.2 cm in diameter. The sputtering chamber was a borosilicate glass bell jar which was oil diffusion pumped and liquid nitrogen trapped. The system base pressure was less than $1x10^{-6}$ torr. The sputtering gases, ultra high purity nitrogen and argon, were leaked continuously at about 20.0 scc/m into the system. A throttle valve, between the liquid nitrogen baffle and the diffusion pump, enabled the diffusion pump to operate at a pressure lower than the sputtering pressure so as to minimize backstreaming. The total gas pressure was regulated with a controller system based on a piezoelectric leak valve. The relative proportions of the sputtering gases was determined with a mass spectrometer.

The silicon nitride was deposited from a commercially obtained high purity pressued powder silicon nitride target. The hafnium nitride was deposited from a hafnium metal target which was 97.48 percent hafnium 2.45 percent zirconium with the balance as assorted low level impurities.

Silicon nitride was deposited at 2 total pressures, 8 and 20 mtorr in a gas mixture of 25 percent (atomic) nitrogen in argon ($f = 0.25$). The mole fraction of nitrogen in argon is defined to be f. Hafnium nitride was deposited at the same two total pressures with $f = 0.25$ and $f = 0.60$. The dc self-bias voltages of the targets were measured, table I. Typical deposition rates were from 150 to 190 Å/min.

The nominal composition of the 440C stainless steel substrates is given in table II. The substrates were in the form of disks 1.0 cm in diameter and 1.6 mm thick. All substrates were hardened to between 53 and 55 Rockwell C by heating to 870 degrees centigrade for 15 min. followed by an oil quench. After hardening all substrates were polished with 1 micron diamond paste and ultrasonically cleaned in Alconox, acetone and 190 proof ethyl alcohol. Some of the substrates were then oxidized by heating, in air, at 350 degrees centigrade

for 17 hours. The hardness of the oxidized substrates was measured to be 50 Rockwell C. The same cleaning procedure was followed after oxiding.

During deposition the substrate to target distance was 32.5 mm for silicon nitride and 37.5 mm for hafnium nitride.

In order to determine the thickness of the coating, a step was formed on a glass slide, by masking, and its height measured with a stylus profilometer.

A scanning electron microscope and windowless energy dispersive X-ray analysis system, was used to study the morphology and composition of the coatings and the substrates.

X-ray diffractometry was used to identify the phases. For this purpose the coatings were deposited on aluminum foil substrates which, in order to promote crystallization, were thermally insulated from the base plate of the sputtering system.

The composition of the coatings and the variation of composition through the interface between the coating and substrate was studied by Auger electron spectroscopy (AES). AES measurements were performed in a baked UHV system which was ion pumped to $<2\times10^{-10}$ torr then backfilled to 4×10^{-5} torr with ultra high purity argon. The AES system consisted of a single pass cylindrical mirror analyzer containing a coaxial electron gun. The gun was operated at a beam current of 2 μamps and at a voltage of 2 kV. The electron beam was 0.3 mm in diameter. The detection system was operated in the first derivative mode using a modulation amplitude of ±5 eV. Auger spectra were obtained while the films were being ion beam milled (sputtered) with 3 kV argon ions. The ion beam was rastered over an area 3 mm by 8 mm. A sputter rate of 13 Å/min was typical under these conditions. The system was interfaced with a microcomputer which swept the pass energy over a preselected set of Auger peaks and recorded the peak to peak amplitudes as a function of time (dose). In this way depth profiles were taken and stored for later manipulation. Data was taken until only the characteristic lines of the substrate remained and their amplitudes became independent of dose. For all samples, the carbon KLL (272 V), nitrogen KLL (381 V), oxygen KLL (510 V), chromium LMM (529 V), and the iron LMM (651 V) lines were recorded. As appropriate, the hafnium NNN (168 V) or the silicon LMM (92 V) lines were also monitored.

The apparatus, shown in figure 2 (taken from ref. 11), was used to measure the friction coefficients. The rider was a ball of 440C stainless steel 7 mm in diameter and hardened to 47 Rockwell C. The friction was measured at a normal load of 100 grams (0.0102 N) under lubricated conditions. A light mineral oil, which had a viscosity of between 19.3 and 21.6 centistokes, was used in all tests.

The microhardness was measured with a Knoop indenter at loads of 10 and 25 grams.

The relative adhesion of the films to the substrates was studied by means of a scratch test. The scratches were produced by sliding a loaded spherical diamond indentor with a radius of 86 microns over the surface. The tracks were examined in the scanning electron microscope (SEM). The critical load was defined as that load at which the coating appeared, in the SEM, to crack.

RESULTS AND DISCUSSION

Morphology

Figure 3 presents SEM micrographs of the substrates prior to deposition. As seen in figure 3(a), the substrate is featureless, except for some fine polishing marks. This is in contrast to the surface of the oxidized substrate, figure 3(b), whose surface is clearly roughened. The dark areas are found, by X-ray analysis, to be rich in chromium and carbon and are most probably chromium carbide formed during the heat treatment. Figures 4 to 6 are SEM micrographs of coatings deposited under various conditions. They were taken of coatings which had broken in the scratch test and were chosen so that both the top and side morphology can be seen. Figure 4 shows a morphology which is typical of both materials as deposited on unoxidized substrates. These coatings are smooth and reproduce the geometric features (scratches, etc.) of the substrates. The side view suggests that the coating failed with a brittle fracture. The morphology of silicon nitride as deposited on the oxidized 440C is shown in figure 5. Figure 5(a) shows a coating deposited at 8 mtorr and figure 5(b) shows one deposited at 20 mtorr. While the surface of the coating in figure 5(a) is rougher than that of the coating deposited on an unoxidized substrate (fig. 4), the general appearance is the same. In contrast, figure 5(b) shows a well defined columnar structure, the caps of which appear as spherical bumps on the surface.

The formation of the columnar structure is expected to occur during sputter deposition on rough substrates at low substrate temperatures (refs. 12 and 13). Under these conditions the arriving atoms are incorporated into the coating close to their points of impact. Therefore shadowing can play an important role in the growth of the coating. Peaks will "see" a higher flux than the valleys if a significant transverse component of velocity is present (ref. 13). The shadowing effect is more pronounced when the mean free path (λ) is short and the characteristic surface roughness is large. At low sputtering pressures (8 mtorr) the dense structure shown in figure 5(a) is obtained. At 20 mtorr the scattering of the sputtered particles from the sputtering gas atoms increases (smaller λ), increasing the size of the transverse component of the coating flux, resulting in the columnar structure.

The morphology of the hafnium nitride coatings deposited on an oxidized substrate at 8 mtorr is similar to that of silicon nitride deposited under the same conditions (see fig. 5(a)). Figure 6 shows a hafnium nitride coating deposited on an oxidized substrate at 20 mtorr. It has a dense structure similar to that of silicon nitride deposited at 8 mtorr (see fig. 5(a)). The failure of the hafnium nitride coatings to develop the columnar structure, seen in silicon nitride when deposited at the same pressure, may be related to the higher self-bias (see table I). It has been shown (refs. 14 and 15) that this will lead to higher energy sputtered atoms and incomplete thermalization. This implies that the hafnium atoms are not only more mobile but, on arrival at the substrate, have a smaller average transverse component of velocity. Both these conditions are expected to lead to a reduced tendency to develop a columnar structure.

Crystal Structure

The X-ray diffractometer data for the silicon nitride coatings showed no evidence of crystallinity. The hafnium nitride films however did exhibit broad peaks consistent with crystallites with a characteristic linear dimension of at least 50 Å. The diffraction pattern in all cases suggested mixed phases of NfN and Hf_4N_3. The coatings deposited with $f = 0.60$ were predominately HfN while those deposited with $f = 0.22$ were predominately Hf_4N_3.

AES: Silicon Nitride

In figure 7 is shown a series of AES spectra (50 to 1000 eV) which are typical of the silicon nitride coatings studied here. The spectrum (A) of an "as deposited" sample has features corresponding to the LMM lines of silicon and the KLL lines of carbon, oxygen and nitrogen. After sufficient ion milling to remove the surface layers the argon LMM line also appears (B). The ion milling also has another effect in that the energy of the major silicon line increases from 85 to 92 eV, an energy more typical of elemental silicon. This behavior has been observed previously (refs. 16 and 17) and has been interpreted as an electron and/or ion beam induced decomposition of the nitride. This interpretation is consistent with both the shift in energy and the change in the silicon line shape observed in this work. In table III are shown the elemental amplitudes normalized to the silicon peak. Also shown are the deposition pressures and the normalized nitrogen amplitude for Si_3N_4 as reported by McGuire (ref. 18) and corrected to the 2 kV electron energy used for this work. It is clear from this table that from the point of view of coating purity and stoichiometry the lower (8 mtorr) deposition pressure is associated with the better films. They only have nitrogen to silicon ratios significantly closer to Si_3N_4 but show a carbon contamination level approximately 1/2 of that of the 20 mtorr samples. The oxygen contamination is also lower by about a factor of 3 in these samples.

Figure 8 shows a depth profile of a silicon nitride coating on an oxidized 440C substrate. The profile is a plot of uncorrected peak to peak amplitudes as a function of sputtering time. This profile exhibits a narrow (~50 Å) contaminated surface layer followed by the coating. Next appears a wide interface which contains oxides and mixed phases followed by the substrate. It should be recognized that the apparent width of the interface is certainly greater than the true width. This is primarily due to the non-ideal way in which the ion beam interacts with the sample (ref. 19). The most important resolution limiting effect in this work is undoubtably a geometric one. The ion beam does not mill the surface uniformly over the area of the electron beam (2×10^{-6} mm^2). The surfaces of the samples are rough on this scale with peak to valley dimensions compareable to the coating thicknesses (~1000 Å). Under these conditions the AES signal is a weighted average of spectra from a wide range of depths. Even under the limitations suggested by the above considerations certain consistent behavior is seen. The coatings on the unoxidized substrates show interface widths of 300 Å for the 20 mtorr samples and 150 Å for the 8 mtorr coatings. The interface "width" is defined here as the distance from the point where the silicon amplitude is 0.8 of its bulk value to the point where the iron amplitude is 0.8 of its bulk value. The maximum value of the oxygen peak in this region is approximately the same relative amplitude in both the oxidized and unoxidized cases, however, the samples on

the oxidized substrates exhibited interfaces which were typically twice as wide. The interfaces in all cases are rich, relative to nominal bulk values, in chrome.

AES: Hafnium Nitride

Figure 9 exhibits two Auger spectra. The first (A) is characteristic of the "as deposited" hafnium nitride films and the second (B) is typical of the bulk region, i.e., that exposed after ion milling. The KLL lines of carbon, nitrogen and oxygen and the NNN lines of hafnium are evident. The spectrum of the "as deposited" film, figure 9(a), also shows a sulfur LMM peak, at 152 eV, which disappears after ion milling and is replaced by the argon LMM line. The bulk properties of the coatings are given in table IV, in the form of ratios between the peak to peak amplitudes of nitrogen, carbon and oxygen, and the peak to peak amplitude of the hafnium lines. The deposition pressures and the fraction of nitrogen gas (f) in the sputter gas are also shown. In contrast to the silicon nitride results there is no correlation between either the sputter pressure or f and the impurity levels (O/Hf, C/Hf). A typical depth profile of a film on an oxided substrate is shown on figure 10. As was the case with the silicon nitride all the samples whether, on oxidized substrates or not, showed oxide at the interface. The interface thicknesses, as previously defined, were approximately 600 Å for the oxidized substrates and 300 Å for the unoxidized substrates and were independent of sputtering pressure.

X-ray Analysis

Energy dispersive X-ray analysis (EDXA) of the coatings was used to complement the AES analysis, particularly to establish the existence of entraped argon in the "as deposited" coatings. The relative elemental peak heights were used to provide a qualitative comparison of coatings deposited under different conditions. Figure 11 presents an EDXA spectrum typical of a silicon nitride film deposited at a pressure of 8 mtorr. These films contain, in addition to argon, an oxygen peak which is small relative to the nitrogen peak. The spectrum of the 20 mtorr silicon nitride films, figure 12, indicates that the argon is present but in significantly lower concentrations then in the 8 mtorr film. In agreement with the AES results the oxygen contamination peak is much larger than that observed in the 8 mtorr films. Both spectra, figures 11 and 12, show that some aluminum is incorporated in the silicon nitride films. The aluminum contamination is believed to come from some of the fixturing used in the sputtering system.

The hafnium nitride films also show, figure 13, trapped argon. The ratio of the ArK peak amplitude to the HfM peak amplitude was found for to be independent of the sputtering conditions. The oxygen peak amplitude also exhibited no dependance on the sputtering conditions. It was not possible to verify the existence of aluminum in these samples as it's peak is overlapped by a hafnium peak of high intensity.

The entrapment of argon in sputter deposited coatings has been reported previously and the experimental situation is reviewed in reference 20, where it is shown that the amount of gas incorporated in the film:

(a) Decreases with increasing deposition pressure as the result of a decrease in the plasma potential.
(b) Increases with target bias.
(c) Increases with the atomic number of the target.

The occurence of argon, as determined in this study, is generally consistent with the above. For silicon nitride, which was deposited from a relatively low atomic mass target (20 amu), 20 mtorr is apparently a high enough pressure to suppress the entrapment of argon. On the other hand hafnium nitride films, which are deposited from a high mass (178.5 amu) target and at a higher target bias voltage, have argon entrapped at both 8 and 20 mtorr.

Friction Coefficients

Figure 14 presents a typical friction force vs. time curve. The data is characterized by three parameters: the minimum value of the friction coefficient, μ_{min}; the maximum value, μ_{max} and their difference, $\Delta\mu$. No systematic dependence of any of these parameters on the sputtering conditions was observed for either silicon nitride or hafnium nitride. The average value of these coefficients are given in table V. The coefficients for the uncoated substrates are also given. The data shows that, in the case of the uncoated substrates, the oxidized sample has a significantly higher value of μ_{max} and $\Delta\mu$ than the unoxidized sample. This behavior is consistant with the greater roughness of the sample. In the case of the coated samples both materials show the identical behavior with respect to the difference between the oxidized and unoxidized substrates. That is, in neither case, is there a significant difference in the three friction parameters. For silicon nitride μ_{min}, μ_{max} and $\Delta\mu$ are 0.33, 0.52 and 0.16, respectively. For hafnium nitride the same coefficients are 0.42, 0.73 and 0.26.

Microhardness

Figures 15 and 16 exhibit the microhardness results for silicon nitride and hafnium nitride as a function of the deposition parameters and substrate condition. For comparison, the microhardness of the substrates are also shown. For this test, the silicon nitride coatings were 1.5 microns thick and the hafnium nitride coatings were 1.2 microns thick. It is clear that the apparent microhardness of coatings, as deposited on oxidized substrates, is generally higher than that measured on the same coatings deposited on unoxidized substrates. The microhardness observed for the silicon nitride deposited on an oxidized substrate, at 20 mtorr, is essentially the same as that of the substrate. The apparent microhardness of the films deposited on the unoxidized substrate at 20 mtorr and measured at a load of 10 grams is even less. At a load of 25 grams the films cracked and no measurement could be made. The anomalously low values measured indicate that the films deposited at 20 mtorr have poor adhesion to the substrate. In contrast, a microhardness of 2265 kgm/mm^2 was measured, at a load of 10 gm, for a silicon nitride film deposited at 8 mtorr on an oxidized substrate. For these same conditions, only 1131 kgm/mm^2 was measured for the same material deposited on an unoxidized substrate. This difference, for films expected to have the same bulk properties, is attributed to a difference in the adhesion, between the coating and substrate, in the two cases. The sample with the lower shear strength bond

will be expected to exhibit a lower apparent microhardness with the difference going to zero as the thickness (T) becomes large with respect to the depth of penetration (D) of the indentor. The increased apparent microhardness for the 10 gram loads over the 25 gram loads for the same films indicates that the thickness of these films is not sufficiently large, with respect to the depth of penetration of the indentor, to give true bulk values. Some values of D/T are shown, figure 15, at the tops of the bars. D/T is defined as the ratio of the penetration depth of the indentor to the thickness of the coating. In an attempt to observe a hardness closer to the bulk value some thicker silicon nitride films were prepared. The microhardness data for these are given in table VI. The 2.3 micron thick sample deposited on the oxidized substrate exhibits a Knoop hardness of 3900±500 kg/mm^2 when subjected to a 10 gram load. The D/T is, in this case, less than 0.1. It has been shown (ref. 21) that this is a condition under which the true bulk value would be observed. It is, within experimental error, in agreement with a previously reported (ref. 22) value of 3260 kg/mm^2. It is clear that 3900±500 kg/mm^2, as measured here, can only be considered a lower limit for these films.

The microhardness data for the hafnium nitride coating is summarized in figure 16. Some representative values of D/T are indicated above the bars. They are also in the range where interfacial strength and substrate properties are expected to influence the results. Therefore the hardness values shown must, as in the silicon nitride case, be taken as lower limits to the true bulk value. The highest value (1650 kg/mm^2) is associated with the sample deposited at 8 mtorr with $f = 0.25$ on an oxidized substrate. Previously reported values (ref. 23) of between 1480 and 1800 kg/mm^2 are in agreement with the highest values seen in this work. Some of the samples deposited at 20 mtorr on unoxidized substrates have an apparent hardnesses less than that of the substrate indicating very poor adhesion.

Scratch Tests

SEM micrographs of typical scratches are shown in figures 17 and 18 for silicon nitride and hafnium nitride, respectively. They are seen to be somewhat different. At the critical load (100 gm), figure 17(a), the silicon nitride exhibits evidence for brittle failure and poor interfacial adhesion. The coating is seen to break away, along the track, from the substrate. At 200 gm, twice the critical load, figure 17(b), the substrate is completely exposed with only small scratched pieces of the coating visable in the track. The micrograph of a typical hafnium nitride coating subjected to its critical load (200 gm), figure 18(a), also shows some cracking and flaking at the edges of the track however, in the track, it appears to behave ductily and remains bonded to the substrate. Figure 18(b) shows a hafnium nitride coating on an unoxidized substrate which was subjected to a load greater than three times its critical load. Even under these sever conditions it remains in the track.

Figures 19 and 20 present the critical load data for the two materials. It can be seen that the critical load is always higher for films deposited on oxidized substrates and further that deposition at the lower pressure (8 mtorr) is superior to deposition at the higher pressure (20 mtorr) for adhesion. For silicon nitride the critical load is almost twice that measured on the unoxidized substrates. The critical load is lowest for the 20 mtorr films and is practically zero for hafnium nitride on unoxidized 440C. A maximum critical

load of 150 gm is measured for silicon nitride deposited at 8 mtorr on oxidized 440C. This is significantly lower than the maximum (250 gm) measured for the hafnium nitride films deposited at the same pressure on the same substrates with $f = 0.6$. It should be recalled that not only is this material softer than the silicon nitride but is softer than the hafnium nitride deposited at $f = 0.25$. Although is difficult to directly compare the two materials with respect to their behavior in this test, it does appear that the oxide has a larger effect on the adhesion in the case of silicon nitride than it has on the adhesion of the hafnium nitride. This behavior is made plausible if the thermal contribution to the interfacial stresses is examined. Table VII gives some literature values for the coefficients of thermal expansion for the coatings, substrate and some mixed chrome and iron oxides. Although amorphous silicon nitride will have a coefficient different from the crystalline material, it is still expected to be much smaller than that of 440C. Therefore, it must follow that shear stresses will develop at the interface as the sample cools to room temperature after the deposition. Assuming similar thermal histories, their relative thermal expansion coefficients and hardnesses, higher interface stresses are expected for silicon nitride than for hafnium nitride. The AES depth profiles show that the oxides at the interface are chrome rich relative to the bulk alloy and are, as expected, much thicker on the oxidizer substrates. If either of the mixed oxides of table VII are a reasonable approximation to the chemistry at the interface, then the success of the oxide in improving adhesion may be partly the result of the fact that its thermal expansion is intermediate between the coating and the substrate. This and its relative mechanical weakness will aid adhesion by grading the mechanical mismatch over a many more atomic layers.

CONCLUSIONS

1. The coatings deposited on unoxidized substrates have a dense smooth structure reproducing the features of the substrate. Those deposited on the oxidized substrates have the rougher morpohology. Only the silicon nitride deposited, at 20 mtorr, on oxidized substrates had a columnar structure. This is apparently due to the high "effective roughness" resulting from the combination of a short mean free path and the low atomic mass of the silicon nitride target.

2. The silicon nitride coatings were found to be amorphous while the hafnium nitride films showed evidence of crystallinity with a grain size of at least 50 Å.

3. X-ray diffractometry suggests that the hafnium nitride coatings are a mixture of phases. Those deposited with $f = 0.6$ were predominately HfN while the films deposited with $f = 0.2$ showed the lines, corresponding to Hf_4N_3, to be more intense. This is consistent with the AES results which showed that the films deposited at the higher value of f were richer in nitrogen.

4. Silicon nitride showed significantly higher impurity levels (oxygen and carbon) than the hafnium nitride. This may be the result of outgasing from the pressed powder target used for the silicon nitride.

5. Argon was found, except for the silicon nitride deposited at 20 mtorr, in all films.

6. The friction coefficient, relative to hardened 440C steel, ranged from 0.33 to 0.56 for silicon nitride and from 0.42 to 0.73 for hafnium nitride.

7. Microhardnesses of 1650±100 kg/mm^2 and 3900±500 kg/mm^2 were measured for the best hafnium nitride and silicon nitride coatings, respectively. These values are in agreement with the bulk values quoted in the literature however they are only lower limits for these coating.

8. Adhesion of both silicon nitride and hafnium nitride to hardened 440C steel, as measured by the critical load of the scratch test, is improved by a reduced sputtering pressure and by preoxidizing the substrates. The hafnium nitride exhibits ductile failure and remains in the track at loads well above the critical load. This is in contrast to silicon nitride, which shows evidence of brittle failure and does not stay in the track at loads significantly above critical.

REFERENCES

1. Engineering Property Data on Selected Ceramics. Vol. I: Nitrides. MCIC-HB-07-VOL-1, Battelle Columbus Labs., 1976. (AD-A023773.)
2. Sekimoto, M.; et al.: Silicon Nitride Single-Layer X-Ray Mask. Jpn. J. Appl. Phys., vol. 20, no. 9, Sept. 1981, pp. L669-L672.
3. Leigh, P. A.: Investigation of CVD Silicon Nitride Encapsulation for Gallium Arsenide. Int. J. Electron., vol. 52, no. 1, Jan. 1982, pp. 23-41.
4. Tomita, T.; Kasai, I.; and Koshiki, T.: Watch Cases Jap Patent No. A7630525, Apr. 20, 1971.
5. Hezel, R.; and Schorner, R.: Plasma Si Nitride - A Promising Dielectric Achieve High-Quality Silicon MIS/IL Solar Cells. J. Appl. Phys., vol. 52, no. 4, Apr. 1981, pp. 3076-3079.
6. Leverenz, R. V.: Look at the Hafnium Nitride Coatings. Manuf. Eng., vol. 79, no. 1, July 1977, pp. 38-39.
7. Kodama, M.; Shabaik, A. W.; and Bunshah, R. F.: Machining Evaluation of Cemented Carbide Tools Coated with Hf and TiC by the Activated Reactive Evaporation Processes. Thin Solid Films, vol. 54, 1978, pp. 353-357.
8. Grill, A.; and Aron, P. R.: Sputtered Silicon Nitride Coatings for Wear Protection. Thin Solid Films, vol. 96, no. 1, Oct. 1, 1982, pp. 25-30.
9. Aron, P. R., and Grill, A.: Some Properties of R. F. - Sputtered Hafnium Nitride Coatings. Thin Solid Films, vol. 96, no. 1, Oct. 1, 1982, pp. 87-91.
10. Brainard, W. A.: The Friction and Wear Properties of Sputtered Hard Refractory Compounds. NASA TM-78895, 1978.
11. Miyoshi, K.; and Buckley, D. H.: Friction and Surface Chemistry of Some Ferrous-Base Metallic Glasses. NASA TP-1991, 1982.
12. Thornton, J. A.; Tabock, J.; and Hoffman, D. W.: Internal Stresses in Metallic Films Deposited by Cylindrical Megnetron Sputtering. Thin Solid Films, vol. 64, 1979, pp. 111-119.
13. Thornton, J. A.; and Hoffman, D. W.: Stress-Related Effects in Thin Films. Proceedings of the 22nd Annual Technical Conference of the Society of Vacuum Coaters. Society of Vacuum Coaters, 1979, pp. 5-18.
14. Wu, C. T.; Kampwirth, R. T.; and Hafstrom, J. W.: High-Rate Magnetron Sputtering of High T_c Nb_3Sn Films. J. Vac. Sci. Technol., vol. 14, no. 1, Jan.-Feb. 1977, pp. 134-137.

15. Westwood, W. D.: Calculation of Deposition Rates in Diode Sputtering Systems. J. Vac. Sci. Technol., vol. 15, no. 1, Jan/Feb. 1978, pp. 1-9.
16. Delord, J. F.; Schrott, A. G.; and Fain Jr., S. C.: Nitridation of Silicon III: Auger and LEED Results. J. Vac. Sci. Technol., vol. 17, no. 1, Jan/Feb 1980, pp. 517-520.
17. Van Dostrom, A.; et al.: Quantitative Auger Microanalysis of the Silicon-Oxygen Nitrogen System. J. Vac. Sci. Technol., vol. 20, no. 4, Apr. 1982, pp. 953-956.
18. McGuire, G. E.: Auger Electron Spectroscopy Reference Manual. Plenum Press, 1979.
19. Carter, G.; Gras-Marti, A.; and Nobes, M. J.: Theoretical Assessments of Major Physical Processes Involved in the Depth Resolution in Sputter Profiling. Radiat. Eff. Lett., vol. 62, no. 3-4, July 1982, pp. 119-152.
20. Vossen, J. L.; and Kern, W.: Thin Film Processes. Academic Press, 1978, p. 58.
21. Angus, H. C.: Properties and Behavior of Precious-Metal Electrodeposits for Electrical Contacts. Trans. Inst. Met. Finish., vol. 39, Pt. 1, 1962, pp. 20-28.
22. Engineering Property Data on Selected Ceramics. Vol. I: Nitrides. MCIC-HB-07-Vol-1, Battelle Columbus Labs., 1976. (AD-A023773.), p. 47.
23. Engineering Property Data on Selected Ceramics. Vol. I: Nitrides. MCIC-HB-07-Vol-1, Battelle Columbus Labs., 1976. (AD-A023773.), p. 72.
24. Materials Selection Charts, Martensitic Stainless Steels. Mater. Eng., vol. 96, no. 6, Dec. 1982, p. C39.
25. Shaffer, P. T. B.: Plenum Press Handbooks of High-Temperature Materials. No. 1: Materials Index. Plenum Press, 1964, p. 284.
26. Engineering Property Data on Selected Ceramics. Vol. I: Nitrides. MCIC-HB-07-Vol-1, Battelle Columbus Labs., 1976. (AD-A023773.), p. 71.
27. Shaffer, P. T. B.: Plenum Press Handbooks of High-Temperature Materials. No. 1: Materials Index. Plenum Press, 1964, p. 429.
28. Shaffer, P. T. B.: Plenum Press Handbooks of High-Temperature Materials. No. 1: Materials Index. Plenum Press, 1964, p. 434.

TABLE I. - TARGET BIAS AT 0.5 kW

f	Pressure, mtorr	Target bias, kV	
		Si_3N_4	Hf
0.25	8	1.4	2.2
.60	8	1.4	2.2
.25	20	1.4	2.0
.60	20	1.3	1.9

TABLE II. - COMPOSITION OF 440C STAINLESS STEEL (REF. 24)

Element	C	Cr	Mo	Mn	P	S	Si	Fe
Percent	0.95-1.2	16-18	[a]0.75	[a]1.0	[a]0.04	[a]0.03	[a]1.0	Bal.

[a]Maximum allowed.

TABLE III. - AES PEAK TO PEAK AMPLITUDE RATIOS FOR SILICON NITRIDE

Sample	Pressure, mtorr	Amplitude ratio		
		N/Si	O/Si	C/Si
C40	20	0.89	0.67	0.19
C4	20	.94	.65	.14
B21	22	.94	.88	.15
B19	22	.88	.71	.16
C30	8	.95	.20	.11
C3	8	1.0	.16	.10
D3	8	.98	.30	.07
C50	8	.92	.18	.07
B27	8	.97	.15	.08
Si_3N_4	(ref. 18)	1.0	----	----

TABLE IV. - AES PEAK TO PEAK AMPLITUDE RATIOS

FOR HAFNIUM NITRIDE

Sample	Pressure, mtorr	f	Amplitude ratio		
			N/Hf	O/Hf	C/Hf
Hf1	8	0.25	1.65	0.053	0.19
Hf10	8	.25	2.0	.11	.26
Hf2	8	.60	1.7	.12	.43
Hf20	8	.60	1.4	.09	.29
Hf3	20	.25	2.14	.06	.12
Hf30	20	.25	2.04	.105	.19
Hf4	20	.60	1.75	.08	.29
Hf40	20	.60	1.80	.19	.38

TABLE V. - FRICTION COEFFICIENTS: 440C RIDER

Sample	Substrate	μ_{min}	μ_{max}	$\Delta\mu$
440C	Unoxidized	0.17	0.21	0.03
440C	Oxidized	.19	.42	.23
Silicon nitride	Unoxidized	.33	.52	.16
Silicon nitride	Oxidized	.39	.56	.16
Hafnium nitride	Unoxidized	.42	.73	.26
Hafnium nitride	Oxidized	.42	.69	.25

TABLE VI. - MICROHARDNESS SILICON NITRIDE DEPOSITED

AT 8 mtorr AND f = 0.25

Thickness, T, microns	Substrate	KHN, kg/mm^2			
		at 10 gm	D/T	at 25 gm	D/T
1.3	Unoxidized	1311±100	0.26	1100±60	0.45
1.3	Oxidized	2265±200	.20	1531±100	.38
2.3	Unoxidized	3067±400	.10	2299±80	.17
2.3	Oxidized	3900±500	.09	2520±350	.17

TABLE VII. - THERMAL EXPANSION

Material	Temperature, °C	Thermal expansion, $°C^{-1}$	Reference
440C	0-650	10.9×10^{-6}	24
$Si_3N_4(\alpha)$	25-500	2.1	25
$Si_3N_4(\beta)$	25-500	1.5	25
HfN	0-540	5.4	26
$Cr_2O_3 \cdot FeO$	25-500	8.2	27
$2Cr_2O_3 \cdot Fe_2O_3$	100-200	6.8	28

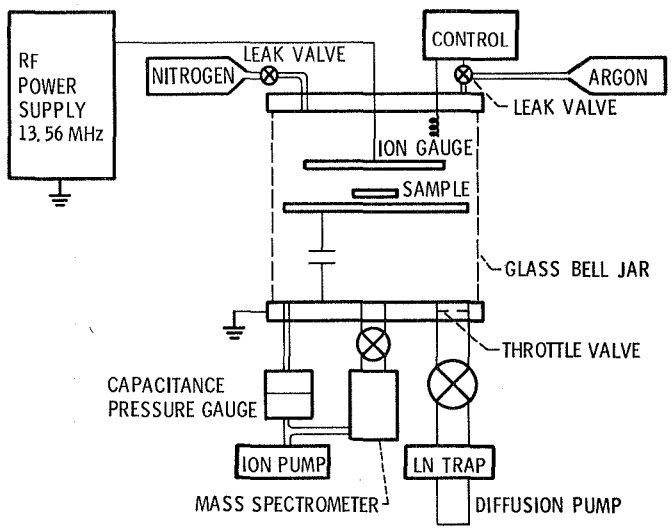

Figure 1. - RF sputtering system.

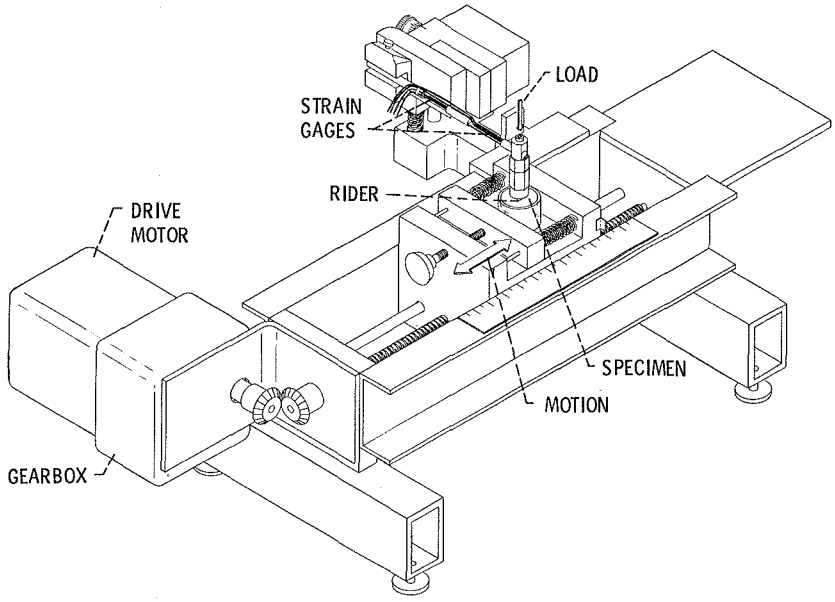

Figure 2. - Friction and scratch test apparatus.

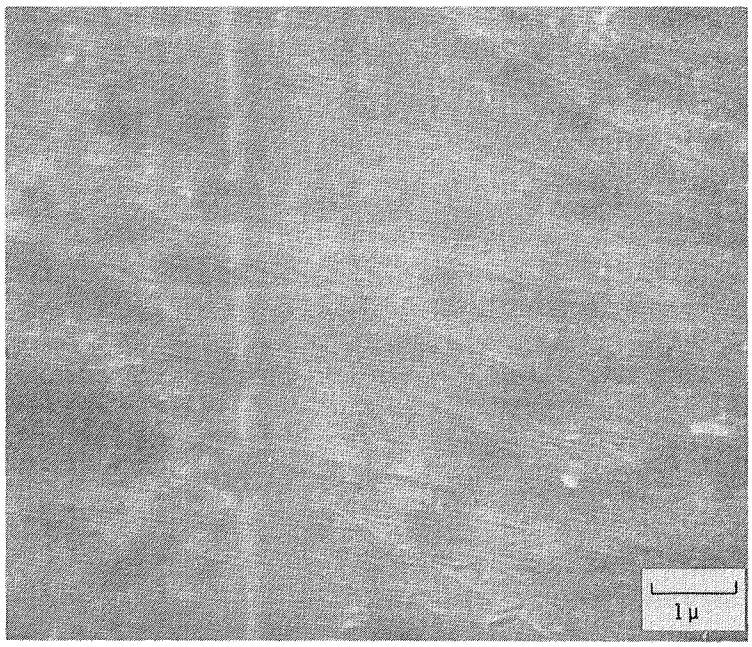

(a) Unoxidized.

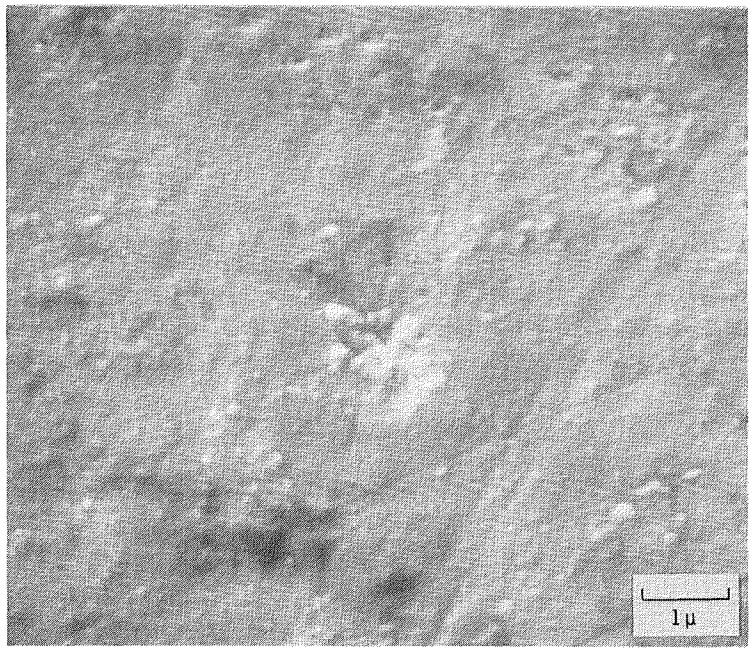

(b) Oxidized.

Figure 3. - SEM micrographs of substrates.

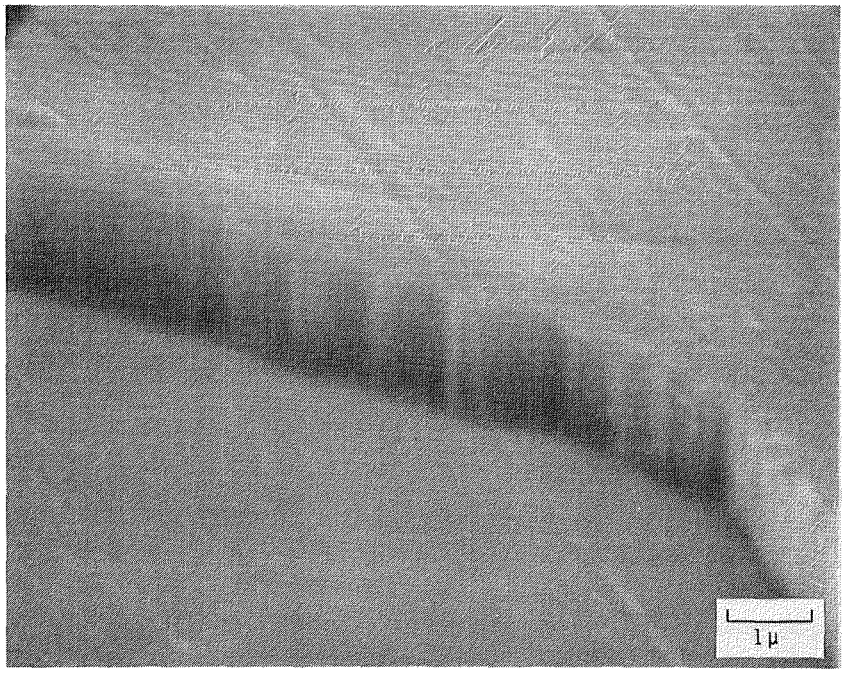

Figure 4. - SEM micrograph: Edge of fractured silicon nitride coating deposited at 20 mtorr on unoxidized 440C.

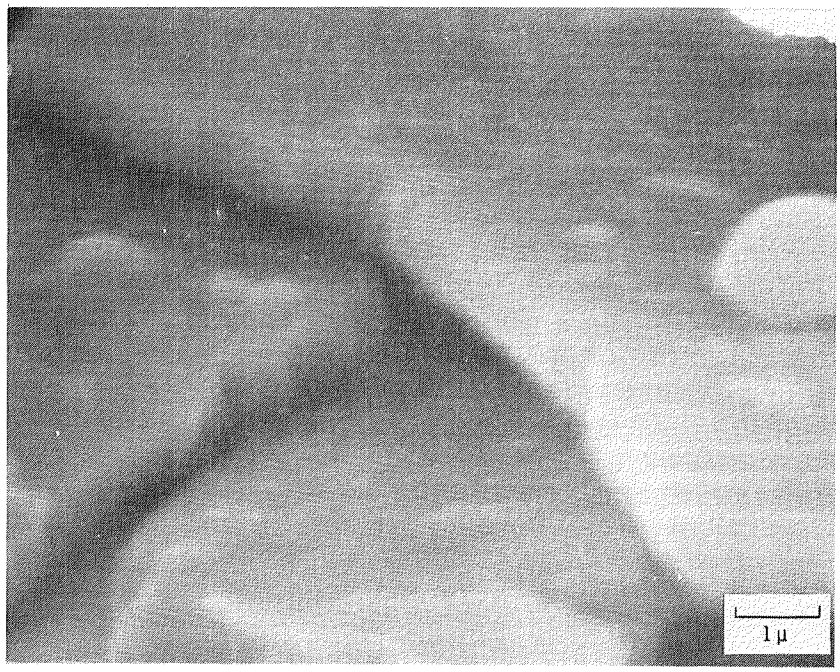

(a) Deposited at 8 mtorr.

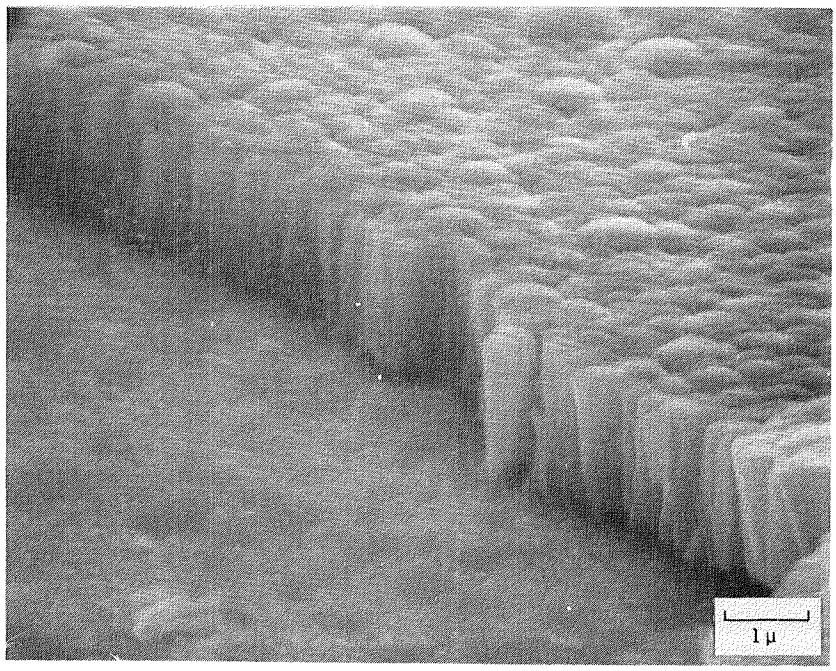

(b) Deposited at 20 mtorr.

Figure 5. - SEM micrographs of silicon nitride on oxidized 440C.

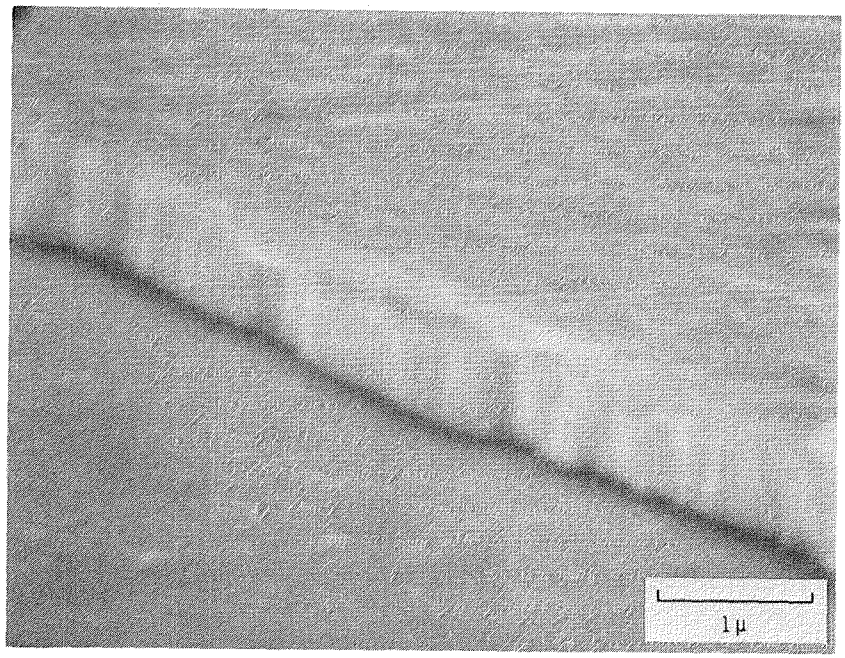

Figure 6. - SEM micrograph: Hafnium nitride deposited at 20 mtorr (f=.25) on oxidized 440C.

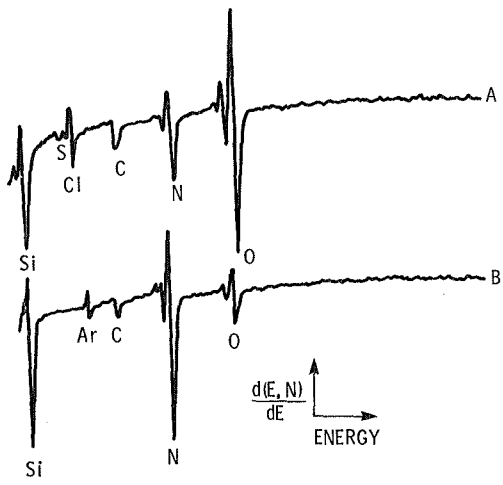

Figure 7. - AES spectrum: As deposited silicon nitride.

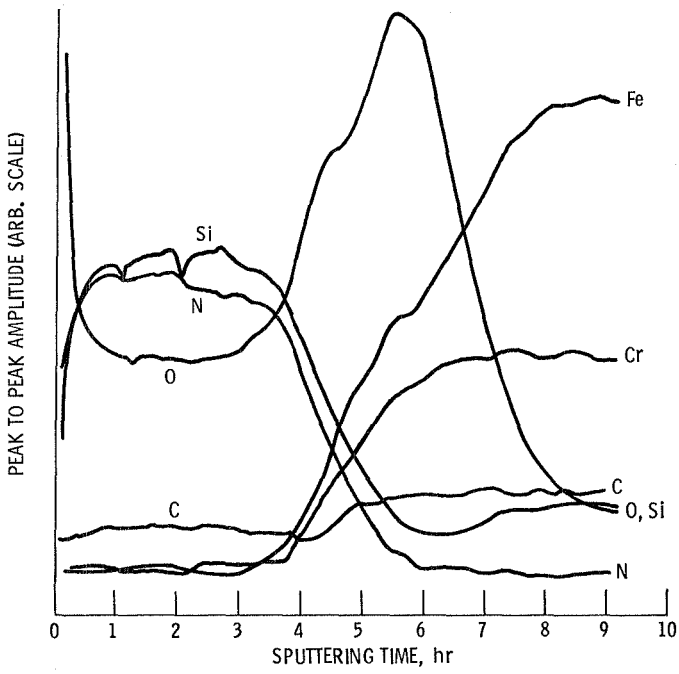

Figure 8. - AES depth profile: Silicon nitride deposited at 20 mtorr on oxidized 440C.

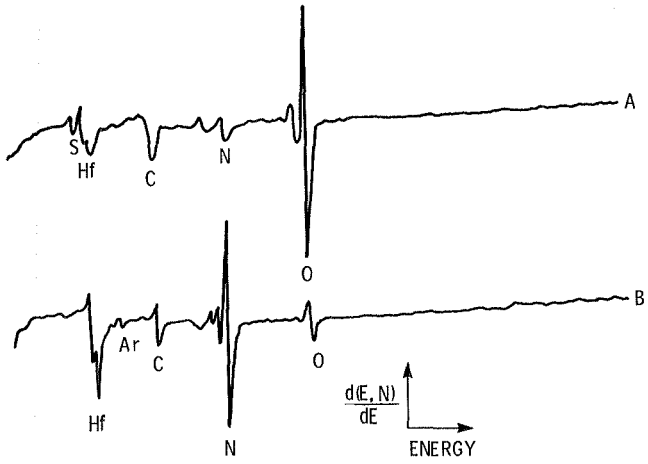

Figure 9. - AES spectrum: As deposited hafnium nitride.

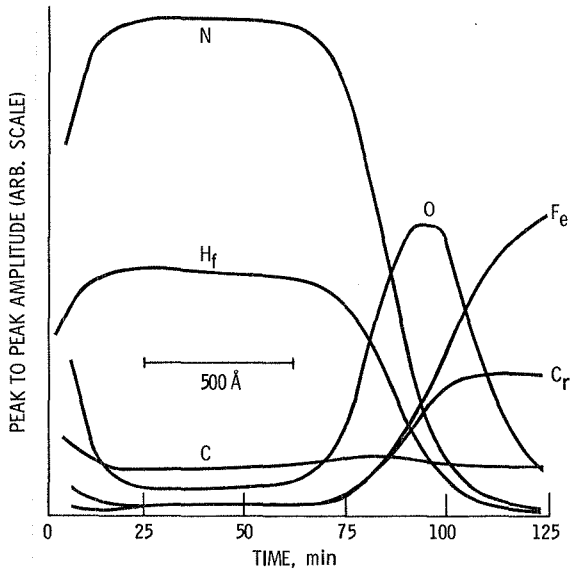

Figure 10. - AES depth profile: Hafnium nitride deposited at 20 mtorr on oxidized 440C.

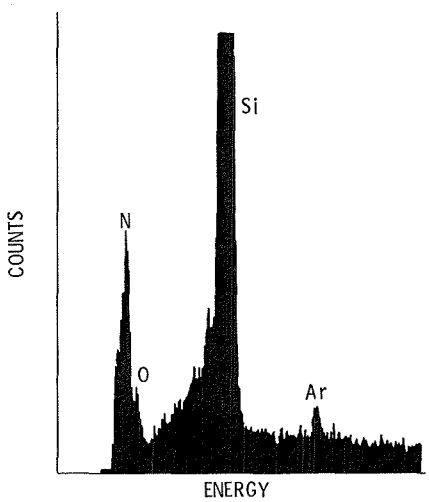

Figure 11. - EDXA spectrum: Silicon nitride deposited at 8 mtorr.

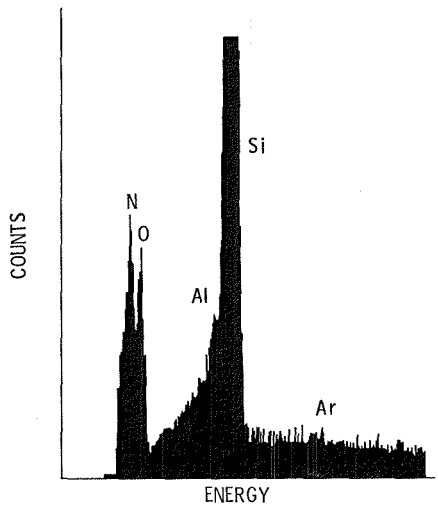

Figure 12. - EDXA spectrum: Silicon nitride at 20 mtorr.

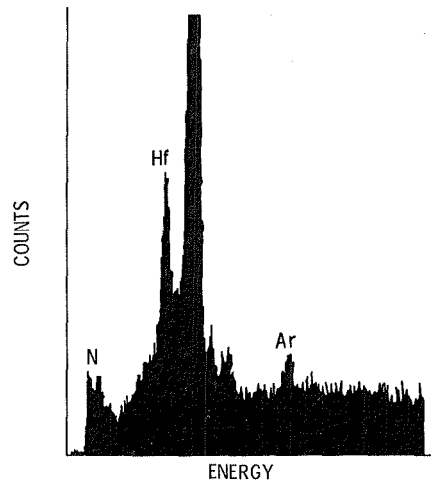

Figure 13. - EDXA spectrum: Hafnium nitride deposited at 8 mtorr (f = 0.25).

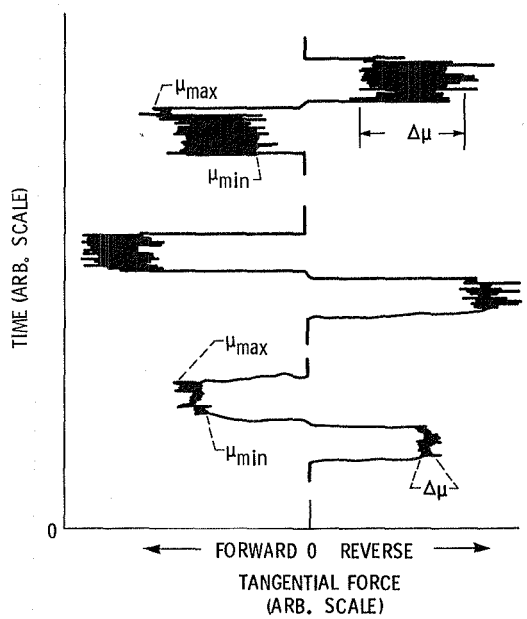

Figure 14. - Typical friction test data.

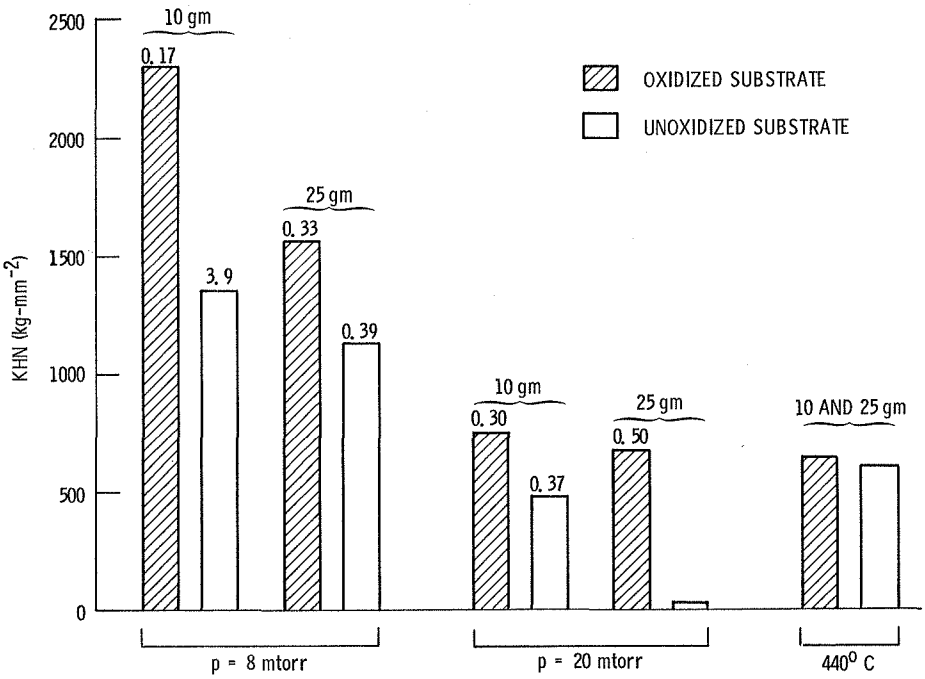

Figure 15. - Hardness: Silicon nitride.

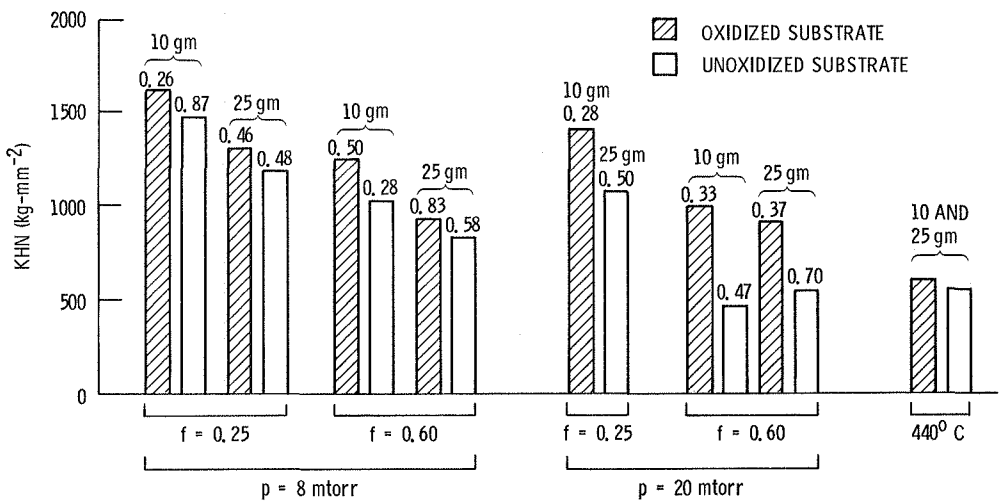

Figure 16. - Hardness: Hafnium nitride.

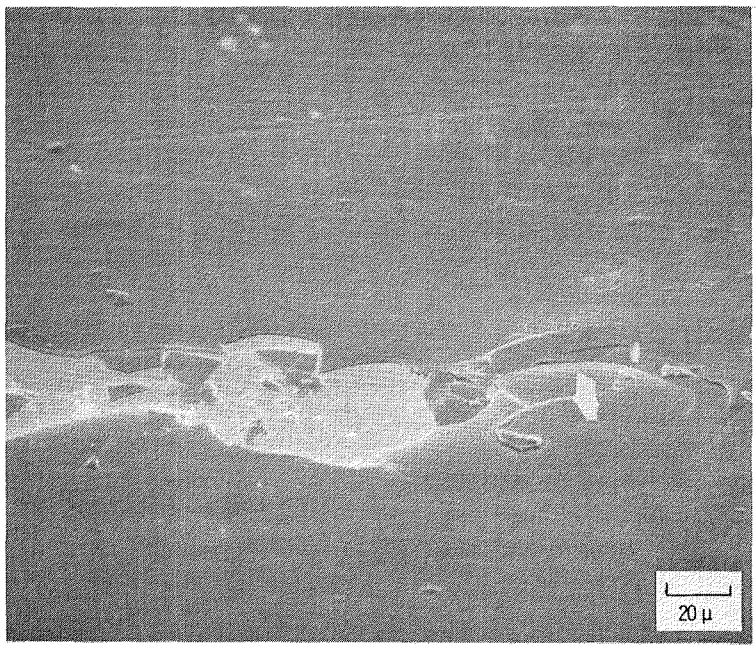

(a) At critical load (100 gm).

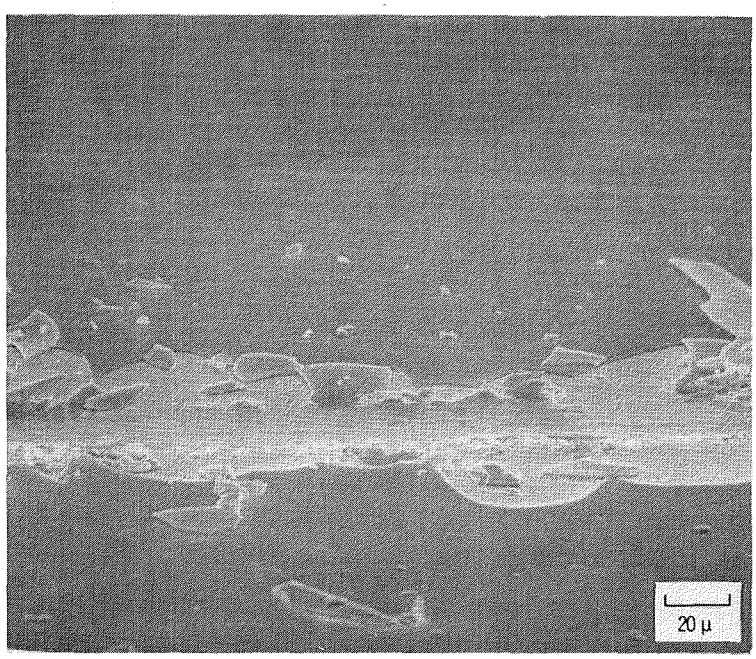

(b) At twice (200 gm) the critical load.

Figure 17. - SEM micrographs of scratches on silicon nitride deposited at 8 mtorr.

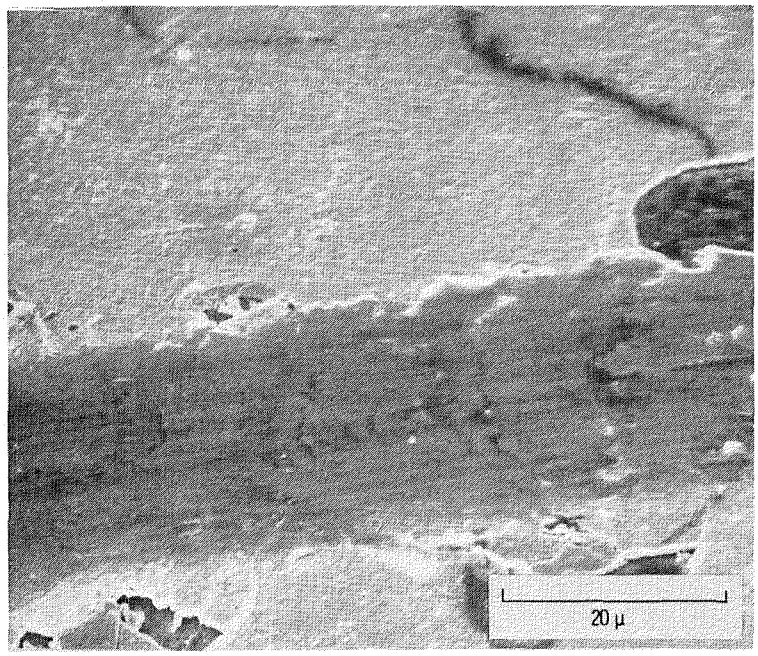

(a) At a 200 gm load on oxidized 440C.

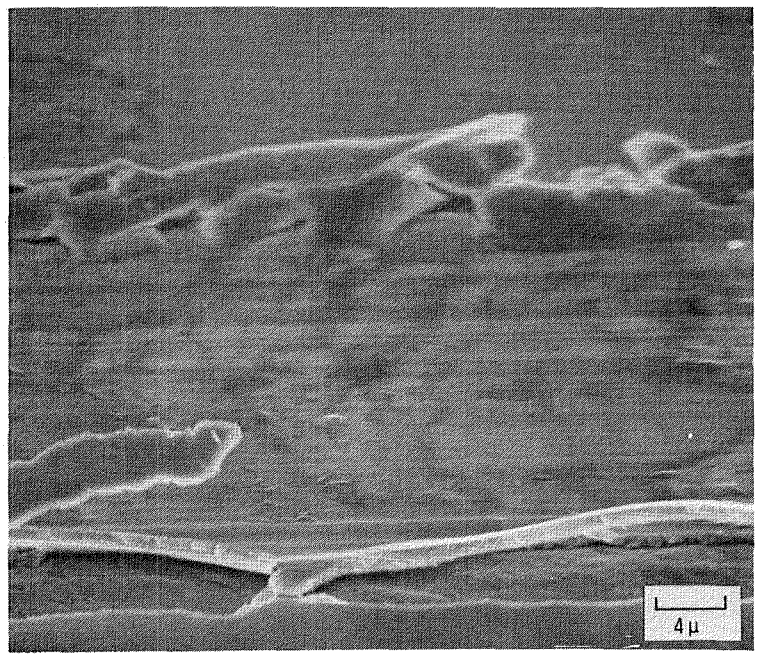

(b) AT (b) At a 550 gm load on unoxidized 440C.

Figure 18. - SEM micrographs of scratches on hafnium nitride deposited at 8 mtorr.

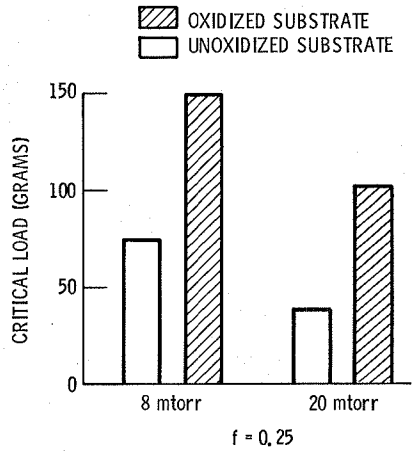

Figure 19. - Critical load versus deposition conditions for silicon nitride on 440C.

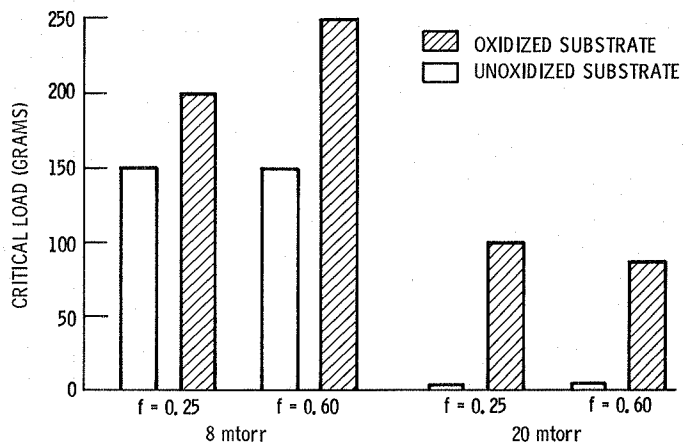

Figure 20. - Critical load versus deposition conditions for hafnium nitride on 440C.

1. Report No.	2. Government Accession No.	3. Recipient's Catalog No.
NASA TM- 86862		

4. Title and Subtitle

RF Sputtered Silicon and Hafnium Nitrides as Applied to 440C Steel

5. Report Date

March 1984

6. Performing Organization Code

506-53-1B

7. Author(s)

A. Grill and P. R. Aron

8. Performing Organization Report No.

E-1993

10. Work Unit No.

9. Performing Organization Name and Address

National Aeronautics and Space Administration
Lewis Research Center
Cleveland, Ohio 44135

11. Contract or Grant No.

13. Type of Report and Period Covered

Technical Memorandum

12. Sponsoring Agency Name and Address

National Aeronautics and Space Administration
Washington, D.C. 20546

14. Sponsoring Agency Code

15. Supplementary Notes

A. Grill, Ben Gurion University of the Negev, Beer Shiva, Israel; P. R. Aron, NASA Lewis Research Center.

16. Abstract

Silicon nitride and hafnium nitride coatings were deposited by reactive rf sputtering on oxidized and unoxidized 440C stainless steel substrates. Sputtering was done in mixtures of argon and nitrogen gases from pressed powder silicon nitride and from hafnium metal targets. Depositions were at two background pressures, 8 and 20 mtorr, and at two different fractions (f) of nitrogen in argon, 0.25 and 0.60, for hafnium nitride and at f = 0.25 for silicon nitride. The coatings and the interface between the coating and substrate were investigated by X-ray diffractometry, scanning electron microscopy, energy dispersive X-ray analysis and Auger electron spectroscopy (AES). A Knoop microhardness of 1650±100 kg/mm^2 was measured for hafnium nitride and 3900±500 kg/mm^2 for silicon nitride. The friction coefficients between a 440C rider and the coatings were measured as lubricated with mineral oil and where found not to depend on the sputtering conditions. They varied between 0.33 and 0.56 for silicon nitride and between 0.42 and 0.73 for hafnium nitride. X-ray diffractometry revealed that the silicon nitride coatings were amorphous. The hafnium nitride coatings were composed of crystallites of mixed phases with a characteristic grain size of no less than 50 Å. The sample with f = 0.60 appeared to be predominately HfN while those with f = 0.25 appeared to be predominately Hf_4N_3. AES showed that the silicon nitride samples deposited at 20 mtorr contained significantly higher levels of oxygen and carbon than the 8 mtorr samples. Oxide was found at all interfaces with an interface width of at least 600 Å for the oxidized substrates and at least 300 Å for the unoxidized substrates. Scratch test results demonstrate that the adhesion of hafnium nitride to both oxidized and unoxidized 440C is superior to that of silicon nitride. Oxidized 440C is found to have increased adhesion, to both nitrides, over that of unoxidized 440C. Coatings of both nitrides deposited at 8 mtorr were found to have increased adhesion to both oxidized and unoxidized 440C over those deposited at 20 mtorr.

17. Key Words (Suggested by Author(s))	18. Distribution Statement
Silicon Nitride Hafnium	Unclassified - unlimited STAR Category 27

19. Security Classif. (of this report)	20. Security Classif. (of this page)	21. No. of pages	22. Price*
Unclassified	Unclassified		

*For sale by the National Technical Information Service, Springfield, Virginia 22161

End of Document